RSC Advances

Effects of hydrogen peroxide on an upward flow biological filter bed (BFB) containing manganese dioxide fillers

Wei Qian[a], Ya Xiong*[a, b], Shuanghong Tian*[a, b], Lianpeng Sun[a, b], Xin Chen[a], Lingjun Kong[a, c], Jialin Zhang[a]

[a] School of Environmental Science and Engineering, Sun Yat-sen University, Guangzhou 510275, China

[b] Guangdong Provincial Key Laboratory of Environmental Pollution Control and Remediation Technology, Guangzhou,510275, P. R. China

[c] School of Environmental Science and Engineering, Guangzhou University, Guangzhou 510006, China

***** E-mail addresses: cesxya@mail.sysu.edu.cn (Y. Xiong).

Highlights:

(a) A lab-scale upward flow BFB with a high decomposition efficiency of H_2O_2 is constructed.

(b) This BFB not only removes the detrimental effect of H_2O_2 but also turns it into DO to boost aerobic microbial metabolism.

(c) A concentration of 120 mg/L H_2O_2 in feed wastewater increases COD removal efficiency by 39%.

Abstract: Generally, there is some residual hydrogen peroxide (H_2O_2) present in treated wastewater from the Fenton and Fenton-like oxidation process. We investigated the influence of residual H_2O_2 on a lab-scale upward flow biological filter bed (BFB) containing manganese dioxide (MnO_2) particles. The H_2O_2 in the feed wastewater was rapidly decomposed into oxygen due to the catalytic role of the MnO_2 particles in the bottom layer of the BFB, resulting in a significant increase in the efficiency of chemical oxygen demand (COD) removal. A concentration of 120 mg/L H_2O_2 in the feed wastewater increased the COD removal efficiency by 39%. This increase can be attributed to the generation of dissolved oxygen (DO) from H_2O_2 decomposition due to aerobic microorganism growth.

Keywords: hydrogen peroxide, biological filter bed, manganese dioxide, dissolved oxygen

1. Introduction

In recent years, Fenton and Fenton-like advanced oxidation technologies have garnered attention due to their treatment efficiency and extensive adaptability [1-4]. However, their high operating costs always perplex wastewater engineers. A frequently used strategy to decrease the cost is to combine Fenton or Fenton-like advanced oxidation with biological technologies [5-10]. In these combination processes, the treated wastewater from the Fenton or Fenton-like reactor usually contains some residual hydrogen peroxide (H_2O_2). However, this residual H_2O_2 has a negative effect on the biological process due to its strong oxidative power [11]. Therefore, a regulation pool is typically built between the Fenton reactors and the biological reactors to remove the residual H_2O_2 [12-14]. H_2O_2 can be catalytically decomposed into H_2O and O_2 by certain metal oxides, as shown in reaction (1) [15-18]. If metal oxide particles are used as the bottom fillers of an upward flow biological filter bed (BFB), H_2O_2 in the wastewater can be decomposed into oxygen as the H_2O_2-containing wastewater flows through the filler layer. Thus, it can be expected that metal oxide filler particles can not only reduce the regulation pool but also provide dissolved oxygen to enhance the growth of microorganisms inside the BFB.

$$2H_2O_2 \rightarrow O_2 + 2H_2O \quad (1)$$

In the paper, a lab-scale upward-flow BFB was constructed, as shown in Fig. 1. In the BFB, MnO_2 particles (0.075~0.15 mm in diameter) were used as catalysts for the reaction (1) because MnO_2 is reported to be an efficient catalyst for H_2O_2 decomposition [19-21]. In this paper, we mainly focus on the effects of H_2O_2 in the BFB. These effects include changes in DO, COD removal, microbial populations and void volume. Our aim was to develop a high efficient Fenton-BFB joint process.

2. Materials and methods

2.1 BFB operation

The experiment was performed in a lab-scale upward-flow BFB. The experiment took place in a greenhouse on SYSU campus in Guangzhou, China. The temperature was in the range of 18-30 ℃. The BFB was constructed using a polypropylene cylindrical container with a diameter of 19 cm and a height of 100 cm, as shown in Fig. 1. The fillers were divided into three layers from the bottom to the top: (i) a 20-cm high pavestone layer with a diameter range of 15 mm-25 mm, (ii) a 50-cm high red brick layer with a diameter of about10 mm and (iii) a 20-cm high river sand layer. All of the containers equipped with valves for sampling in stratified at different substrates. A certain amount of MnO_2 was evenly added to the first layer of the reactor to facilitate H_2O_2 decomposition.

The feed wastewater of the BFB was prepared with glucose ($C_6H_{12}O_6$), ammonium sulfate {$(NH_4)_2SO_4$}, monopotassium phosphate (KH_2PO_4) and water. The COD concentration was 250±20 mg/L. The ammonia concentration was 25±3 mg/L. The total phosphorus concentration was 5.1±0.4 mg/L. The experiment was divided into six stages with different dosages of H_2O_2 (20 mg/L, 40 mg/L, 60 mg/L, 80 mg/L, 120 mg/L and 160 mg/L) under a fixed hydraulic retention time (HRT) of 8 h, flow of 23.6 ml/min, organic loading of 0.3 kg/m^3.d. The experiment was conducted from Mar. 2012 to Oct. 2013.

2.2 Catalytic decomposition of H_2O_2 with MnO_2

The catalytic decomposition of H_2O_2 with various amounts of MnO_2 was conducted in beakers with magnetic stirring at a speed of 100 r/min. In each experiment, a 100-mL solution containing 160 mg/L H_2O_2 was employed.

2.3 Sample analysis

Samples were taken at the A1 (Inlet), A2, A3 and A4 (Outlet) location every two days. The samples were analyzed after filtration. COD was analyzed by the oxidation method using potassium dichromate [22]. The DO in the different layers was measured using a DO (YSI 550A, USA) meter. H_2O_2 concentration was determined by colorimetric methods using titanium oxalate [23]. Microbial populations were observed using a microscope (NMM-820TRF, China).

3. Results and discussion

3.1 Catalytic decomposition of H_2O_2 by MnO_2

Fig. 2 shows the decomposition of hydrogen peroxide with different dosages of MnO_2 at different times. The decomposition efficiency of H_2O_2 was only 3.1% after 60 min when no MnO_2 was added. The decomposition efficiency reached 98% after 60 min when the dosage of MnO_2 was 0.2 g/L. This result confirms that MnO_2 can efficiently decompose H_2O_2. The inset of Fig. 1 presents the change in the decomposition efficiency of 160 mg/L H_2O_2 over 10 min with the addition of MnO_2. The decomposition efficiency of H_2O_2 increased with increasing MnO_2 dosage, reaching a plateau at a dosage of 0.5 g/L. The decomposition efficiency was close to 100%, i.e., the H_2O_2 was completely decomposed. Consequently, the HRT of the wastewater in the MnO_2 catalytic layer was designed to last approximately 10 minutes because 0.5 g/L MnO_2 was sufficient to decompose a concentration of less than 160 mg/L H_2O_2.

3.2 Changes in H_2O_2 and DO concentration in the BFB

The top section of Fig. 3 shows the concentrations of H_2O_2 at various heights of the upward-flow BFB. The H_2O_2 concentrations in the wastewater rapidly decreased with increasing bed height. At a bed height of 20 cm, when the inlet concentration of H_2O_2 was less than 40 mg/L, the residual H_2O_2 was close to zero, i.e., almost all of the H_2O_2 was decomposed in the MnO_2-containing substrate layer at the bottom. Although the inlet concentration of H_2O_2 reached as high as 120 mg/L, the residual H_2O_2 was only 16 mg/L at a height of 20 cm, i.e., the decomposition efficiency was 86.7%. This result indicates that H_2O_2 decomposition is focused at the bottom layer of the upward-flow BFB. As predicted, the H_2O_2 in the wastewater had no negative effect on the growth of the microorganism in the upper parts of the BFB. The vast majority of the H_2O_2 added in the experiment decomposed into H_2O and O_2 as reaction 1, and there was extremely small amounts of H_2O_2 generated $HO_2\cdot$, $O_2\cdot$, and - OH·.

The DO concentration in the BFB also increased, as shown in the bottom section of Fig. 3. Without additional H_2O_2, the DO concentration at the inlet was 8.3 mg/L; however, the DO rapidly decreased with an increase in the height inside the BFB, reaching only 0.4 mg/L at a bed height of 20 cm. This result indicates an anoxic state inside of the BFB. When H_2O_2 was added to the wastewater, the DO concentration inside of the BFB was obviously higher than that without additional H_2O_2, especially when the additional H_2O_2 was above 120 mg/L. At these higher H_2O_2 concentrations, the DO concentration at a bed height of 20 cm reached 15.5 mg/L, indicating a favorable state for aerobic microorganism growth.

According to reaction (1), the oxygen yield should be 0.47 times the H_2O_2 concentration if all of the H_2O_2 is decomposed. Consequently, the oxygenation efficiency (OE) of H_2O_2 decomposition can be calculated with the actual DO data using equation (2).

$$\mathrm{OE}\ (\%) = \mathrm{Increased\ DO}/0.47(\mathrm{addtional\ H_2O_2}\ - \mathrm{residual\ H_2O_2}) \times 100 \qquad (2)$$

As shown in the inset of Fig. 3, the oxygenation efficiencies were 20.9% to 43.8% for feed H_2O_2 concentrations of 20 mg/L to 160 mg/L. The oxygenation efficiency of H_2O_2 was significantly higher than the reaeration rate of atmosphere in the traditional BFB, which generally contains less than 10% oxygen [24], [25]. The high oxygenation efficiency of H_2O_2 is dependent on the characteristics of the liquid oxygen resource. H_2O_2 can be completely mixed with wastewater, homogeneously spread between fillers and is capable of producing pure oxygen. The low oxygenation efficiency of air may be due to the association of oxygen with other gases, such as nitrogen. Thus, H_2O_2 possesses a few advantages as an oxygen resource the Fenton-biological coupling reactor, especially for environments such as wetlands, where aeration is inconvenient.

3.3 Effect of H_2O_2 on COD removal

Fig. 4 shows the changes in COD removal efficiency with H_2O_2 concentration over the course of a stable 60-day run. Without additional H_2O_2, the COD removal efficiency of the BFB was only 40±11% with small fluctuations. The addition of H_2O_2 increased the COD removal efficiency of the BFB. For example, when the wastewater containing 120 mg/L H_2O_2 was fed into the BFB, the mean COD removal efficiency reached 79±8%. This increase was directly proportional to the DO concentration when the concentration of the feed H_2O_2 was below 120 mg/L, as shown in Fig. 5.

Thus, it can be inferred that the increase in COD removal efficiency is due to an enhancement in microbial metabolism due to an increase in the DO rather than from direct oxidation by H_2O_2 and oxygen radicals. It can also be observed from Fig. 5 that the DO in the BFB rapidly increases but that the COD removal does not correspondingly increase when the concentration of the feed H_2O_2 is over 120 mg/L. This result indicates that the DO concentration from the decomposition of 120 mg/L H_2O_2 is sufficient for COD loading. Consequently, the concentration of feed H_2O_2 was controlled below 120 mg/L in the subsequent experiments.

3.4 Changes in void volume

Clogging is a common problem for fixed bed-type reactions. Fig. 6 gives the changes in BFB void volume over 16 months of operation. The void volume decreased from 40.1% to 36.1% after 16 months. This slight decrease suggests that there is no serous clogging. In combination with the results for COD removal, we can infer that the decomposition of H_2O_2 does not cause excessively fast growth of aerobic microorganisms. The microorganisms were observed to exist in aerobic biofilms even with increases in DO in the BFB

3.5 Changes in the microbial populations

Fig. 7 shows images of the microorganism populations for various dosages of H_2O_2 at a bed height of 20 cm during stable operation of the BFB. It can be observed from Fig. 7a that no metazoans were present when the feed wastewater did not contain H_2O_2, which showed that anaerobic and facultative anaerobic bacteria were the dominant populations. However, when the feed wastewater contained 40 mg/L H_2O_2, a larger number of nematodes were observed (Fig. 7b), indicating that the water was in a hypoxic state and that the dominant microbial species were facultative aerobes. When the dosage increased to 80 mg/L, rotifers begin to appear (Fig. 7c), suggesting that the dominant microbial species were aerobic microorganisms. Microscopic analysis showed that H_2O_2 did not have adverse impacts on the growth of microorganisms. This result is because H_2O_2 primarily decomposed at the paving stone layer.

Additionally, as H_2O_2 decomposed and reaeration, the microorganisms at the pavestone layer gradually changed from anaerobic and facultative anaerobic populations to aerobic populations. These observations were consistent with the change in the DO concentration shown in Fig. 2.

3.6 Analysis of economic and application

In China, the cost of conventional BFB for sewage treatment is around 0.5 yuan/m^3. And the cost of industrial H_2O_2 (35% mass fraction) is around 0.8 yuan/kg. The cost of H_2O_2 was 0.27 yuan/m^3, when the feed concentration of H_2O_2 was 120mg/L. The proportion of expense increased by 54%. However, the COD removal efficiency improved from 40% to 79%, the proportion of COD removal efficiency increased to 97.5%. Compared to the increased removal efficiency, the additional cost is acceptable, within a reasonable range. This process has a high economic value.

The improved BFB progress could be widely used in municipal sewage treatment, rural domestic sewage treatment and industrial wastewater deep treatment, due to its remarkable treatment effect, easy operation, on and simple installation. Especially, this progress could combine with Fenton or Fenton-like advanced oxidation technologies, which can not only use the residual H_2O_2 to improve the removal efficiency but also can reduce the cost of H_2O_2.

4. Conclusion

A lab-scale upward flow BFB containing MnO_2 particles was constructed to efficiently decompose H_2O_2 in feed wastewater. The decomposition process not only eliminated the detrimental strong oxidant effect of H_2O_2 but also converted it into DO to boost the aerobic microbial populations, leading to an increase in COD removal efficiency in the BFB. These findings will aid in the development of an efficient Fenton-biological combination process

Acknowledgments

This research was supported by the Nature Science Foundations of China (21107146), Nature Foundations of Guangdong Province (92510027501000005), Science and Technology Research Programs of Guangzhou City (2012J4300118), the Project of Education Bureau of Guangdong Province (cgzhzd1001), and the Fundamental Research Funds for the Central Universities (121pgy20).

References:

[1] A. Aguinaco, F.J. Beltrán, J.J.P. Sagasti, O. Gimeno, In situ generation of hydrogen peroxide from pharmaceuticals single ozonation: A comparative study of its application on Fenton like systems, Chemical Engineering Journal, 235 (2014) 46-51.

[2] A. Gupta, R. Zhao, J.T. Novak, C. Douglas Goldsmith, Application of Fenton's reagent as a polishing step for removal of UV quenching organic constituents in biologically treated landfill leachates, Chemosphere, 105 (2014) 82-86.

[3] M. Munoz, G. Pliego, Z.M. de Pedro, J.A. Casas, J.J. Rodriguez, Application of intensified Fenton oxidation to the treatment of sawmill wastewater, Chemosphere, 109 (2014) 34-41.

[4] N.A. Zubir, C. Yacou, X. Zhang, J.C. Diniz da Costa, Optimisation of graphene oxide–iron oxide nanocomposite in heterogeneous Fenton-like oxidation of Acid Orange 7, Journal of Environmental Chemical Engineering, 2 (2014) 1881-1888.

[5] W. Ben, Z. Qiang, X. Pan, M. Chen, Removal of veterinary antibiotics from sequencing batch reactor (SBR) pretreated swine wastewater by Fenton's reagent,

Water research, 43 (2009) 4392-4402.
[6] E.S. Elmolla, M. Chaudhuri, Combined photo-Fenton-SBR process for antibiotic wastewater treatment, Journal of hazardous materials, 192 (2011) 1418-1426.
[7] Q.Y. Liu, Y.X. Liu, X.J. Lu, Combined Photo-Fenton and Biological Oxidation for the Treatment of Aniline Wastewater, Procedia Environmental Sciences, 12 (2012) 341-348.
[8] R. Nousheen, A. Batool, M.S.U. Rehman, M.A. Ghufran, M.T. Hayat, T. Mahmood, Fenton-biological coupled biochemical oxidation of mixed wastewater for color and COD reduction, Journal of the Taiwan Institute of Chemical Engineers, 45 (2014) 1661-1665.
[9] S. Sanchis, A.M. Polo, M. Tobajas, J.J. Rodriguez, A.F. Mohedano, Coupling Fenton and biological oxidation for the removal of nitrochlorinated herbicides from water, Water research, 49 (2014) 197-206.
[10] S. Sanchis, A.M. Polo, M. Tobajas, J.J. Rodriguez, A.F. Mohedano, Degradation of chlorophenoxy herbicides by coupled Fenton and biological oxidation, Chemosphere, 93 (2013) 115-122.
[11] J.B. Arends, S. Van Denhouwe, W. Verstraete, N. Boon, K. Rabaey, Enhanced disinfection of wastewater by combining wetland treatment with bioelectrochemical H(2)O(2) production, Bioresource technology, 155 (2014) 352-358.
[12] K.V. Padoley, S.N. Mudliar, S.K. Banerjee, S.C. Deshmukh, R.A. Pandey, Fenton oxidation: A pretreatment option for improved biological treatment of pyridine and 3-cyanopyridine plant wastewater, Chemical Engineering Journal, 166 (2011) 1-9.
[13] V.J. Vilar, E.M. Rocha, F.S. Mota, A. Fonseca, I. Saraiva, R.A. Boaventura, Treatment of a sanitary landfill leachate using combined solar photo-Fenton and biological immobilized biomass reactor at a pilot scale, Water research, 45 (2011) 2647-2658.
[14] Q. Xu, A. Hamid, X. Wen, B. Zhang, N. Yang, Fenton-Anoxic–Oxic/MBR process as a promising process for avermectin fermentation wastewater reclamation, Separation and Purification Technology, 134 (2014) 82-89.

[15] V.R. Choudhary, C. Samanta, T.V. Choudhary, Factors influencing decomposition of H2O2 over supported Pd catalyst in aqueous medium, Journal of Molecular Catalysis A: Chemical, 260 (2006) 115-120.

[16] V.R. Choudhary, C. Samanta, P. Jana, Decomposition and/or hydrogenation of hydrogen peroxide over Pd/Al2O3 catalyst in aqueous medium: Factors affecting the rate of H2O2 destruction in presence of hydrogen, Applied Catalysis A: General, 332 (2007) 70-78.

[17] D. Gudarzi, W. Ratchananusorn, I. Turunen, M. Heinonen, T. salmi, Factors affecting catalytic destruction of H2O2 by hydrogenation and decomposition over Pd catalysts supported on activated carbon cloth (ACC), Catalysis Today, (2014).

[18] L. Micoli, G. Bagnasco, M. Turco, M. Trifuoggi, A. Russo Sorge, E. Fanelli, P. Pernice, A. Aronne, Vapour phase H2O2 decomposition on Mn based monolithic catalysts synthesized by innovative procedures, Applied Catalysis B: Environmental, 140-141 (2013) 516-522.

[19] C.A. Páez, D.Y. Liquet, C. Calberg, S.D. Lambert, I. Willems, A. Germeau, J.-P. Pirard, B. Heinrichs, Study of photocatalytic decomposition of hydrogen peroxide over ramsdellite-MnO2 by O2-pressure monitoring, Catalysis Communications, 15 (2011) 132-136.

[20] C. Calberg, M. Deng, G. Ding, S. Chen, F. Xu, Manganese dioxide based ternary nanocomposite for catalytic reduction and nonenzymatic sensing of hydrogen peroxide, Electrochimica Acta, 114 (2013) 416-423.

[21] Y. Li, J. Zhang, H. Zhu, F. Yang, X. Yang, Gold nanoparticles mediate the assembly of manganese dioxide nanoparticles for H2O2 amperometric sensing, Electrochimica Acta, 55 (2010) 5123-5128.

[22] SEPA, Monitoring and Analysis Method of Water and Wastewater, Beijing: China Environmental Science Press, (2002).

[23] R.M. Sellers, Spectrophotometric Determination of Hydrogen Peroxide Using Potassium Titanium(IV) Oxalate, Analyst, 105 (1980) 950-954.

[24] G. Maltais-Landry, R. Maranger, J. Brisson, Effect of artificial aeration and macrophyte species on nitrogen cycling and gas flux in constructed wetlands,

Ecological Engineering, 35 (2009) 221-229.

[25] C. Ouellet-Plamondon, F. Chazarenc, Y. Comeau, J. Brisson, Artificial aeration to increase pollutant removal efficiency of constructed wetlands in cold climate, Ecological Engineering, 27 (2006) 258-264.

Figure Captions

Fig. 1. The BFB experimental system.

Fig. 2. Decomposition efficiency of H_2O_2 (160 mg/L) in the presence of MnO_2.

Fig. 3. Changes in DO and H_2O_2 concentrations at different heights. A1, A2, A3 and A4 are the sampling positions.

Fig. 4. COD removal efficiency at different H_2O_2 concentrations.

Fig. 5. Dependence of COD removal efficiency on H_2O_2 and DO concentrations.

Fig. 6. Changes in the BFB void volume.

Fig. 7. Images of microorganism populations for various dosages of H_2O_2 at a height of 20 cm during the stable running of BFB.

Fig.1

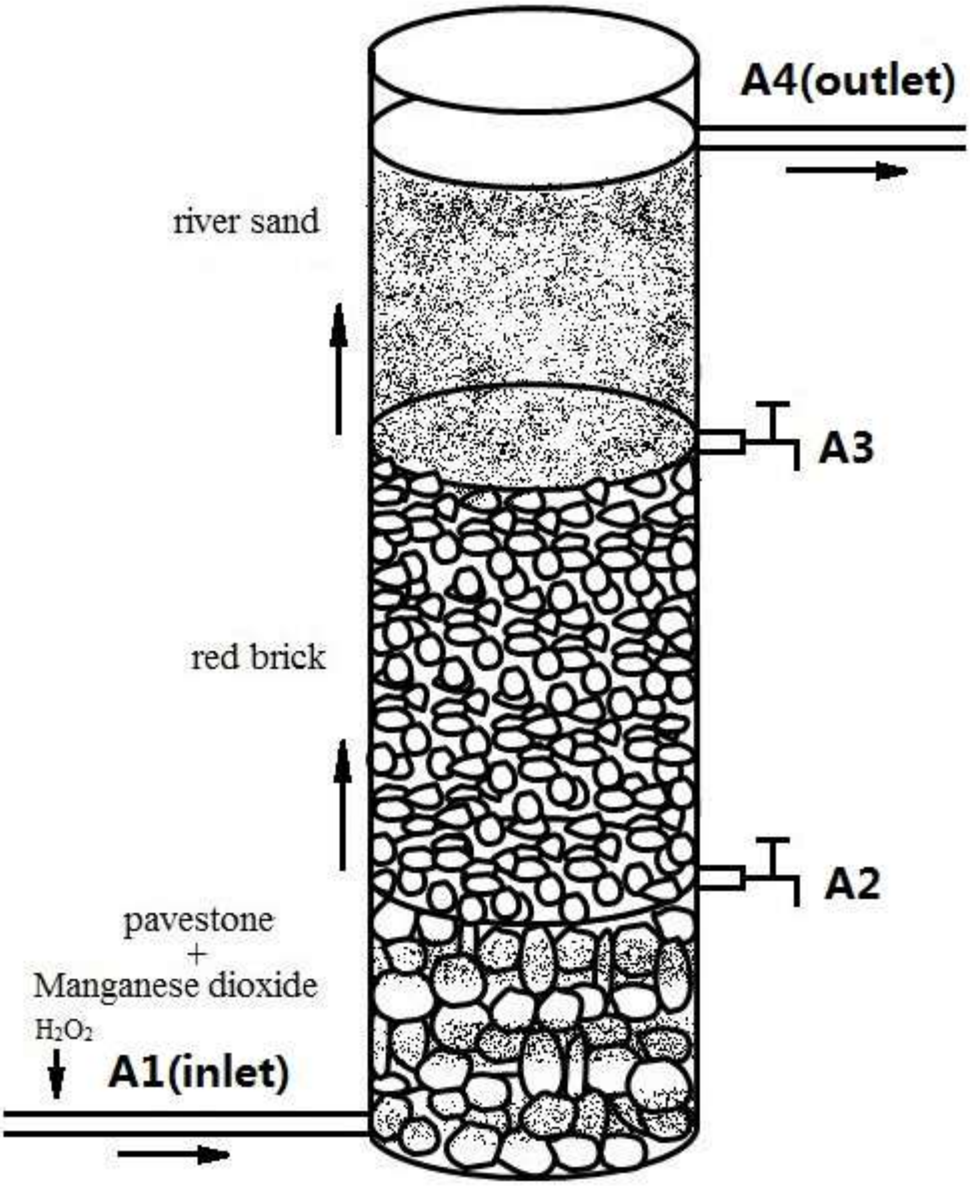
A4(outlet)
river sand
A3
red brick
A2
pavestone
+
Manganese dioxide
H2O2
A1(inlet)

Fig.2

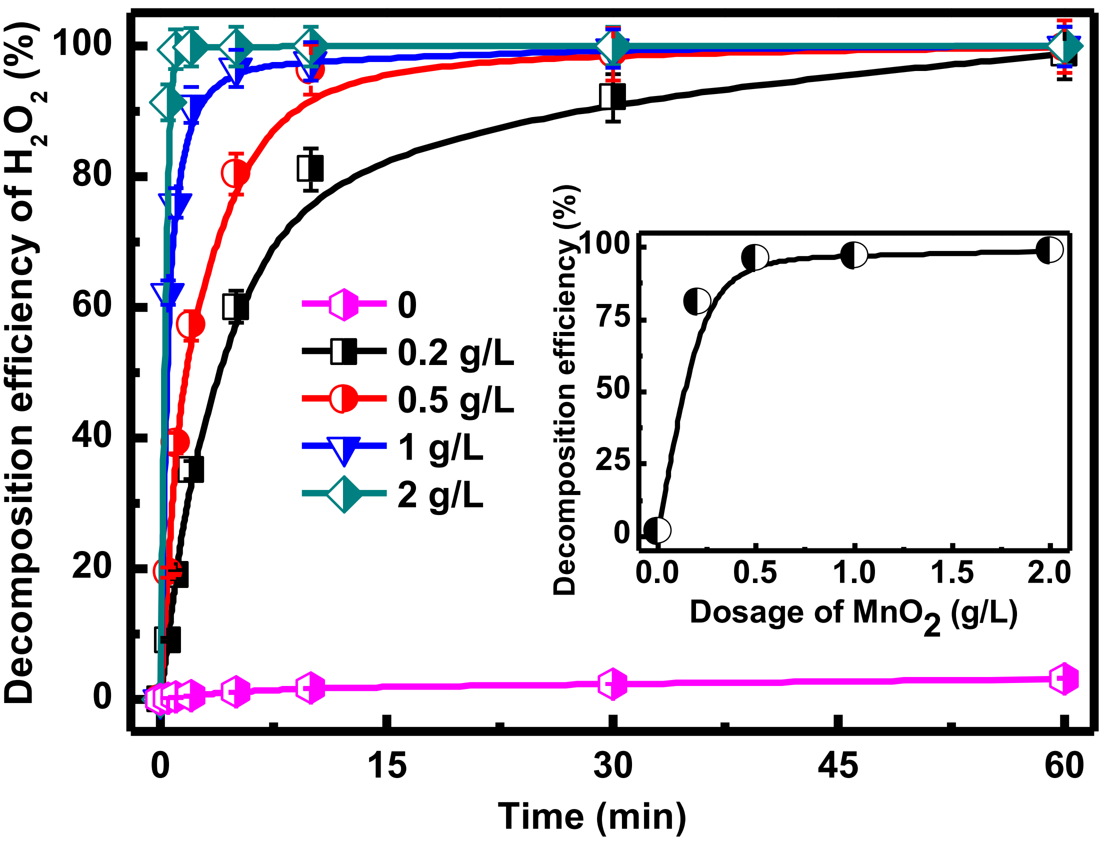
Decomposition efficiency of H_2O_2 (%)
Time (min)
0
0.2 g/L
0.5 g/L
1 g/L
2 g/L
Decomposition efficiency (%)
Dosage of MnO_2 (g/L)

Fig.3

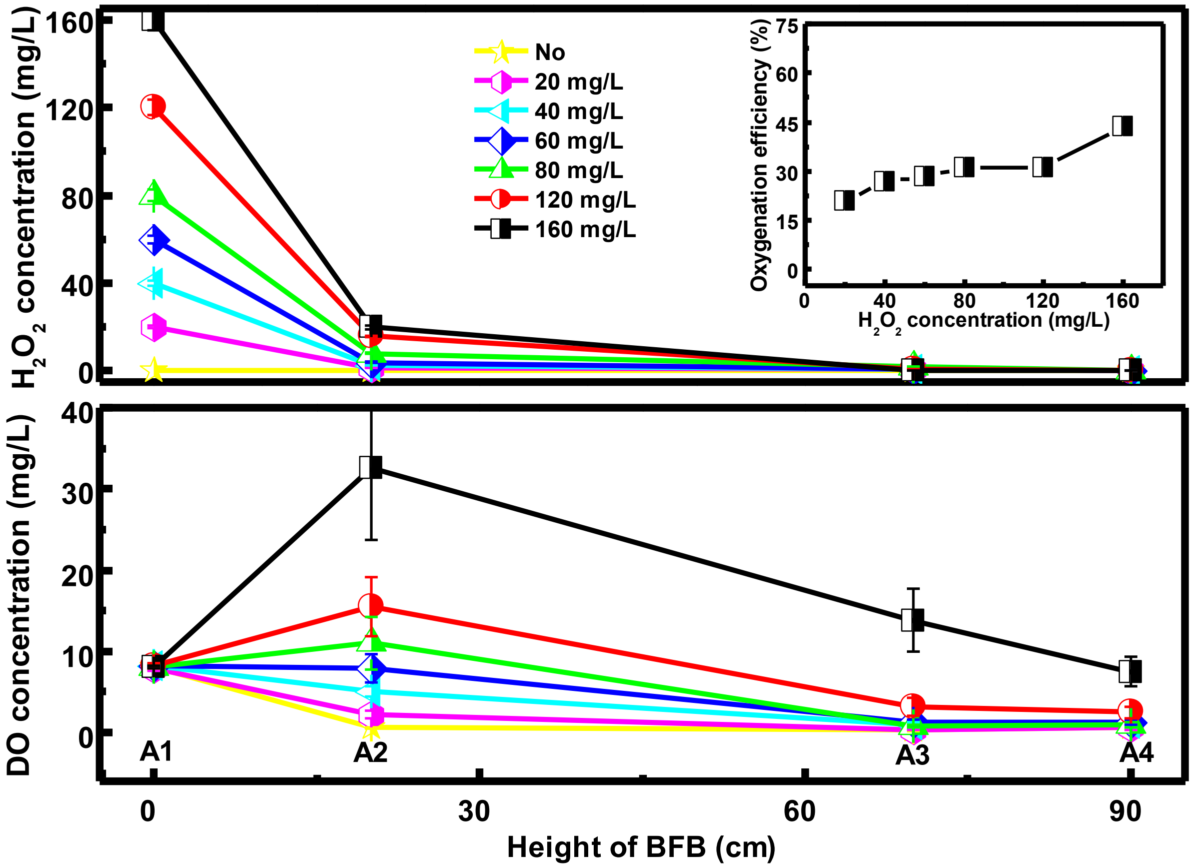

No
20 mg/L
40 mg/L
60 mg/L
80 mg/L
120 mg/L
160 mg/L
H_2O_2 concentration (mg/L)
Oxygenation efficiency (%)
H_2O_2 concentration (mg/L)
DO concentration (mg/L)
A1
A2
A3
A4
Height of BFB (cm)

1 Fig.4

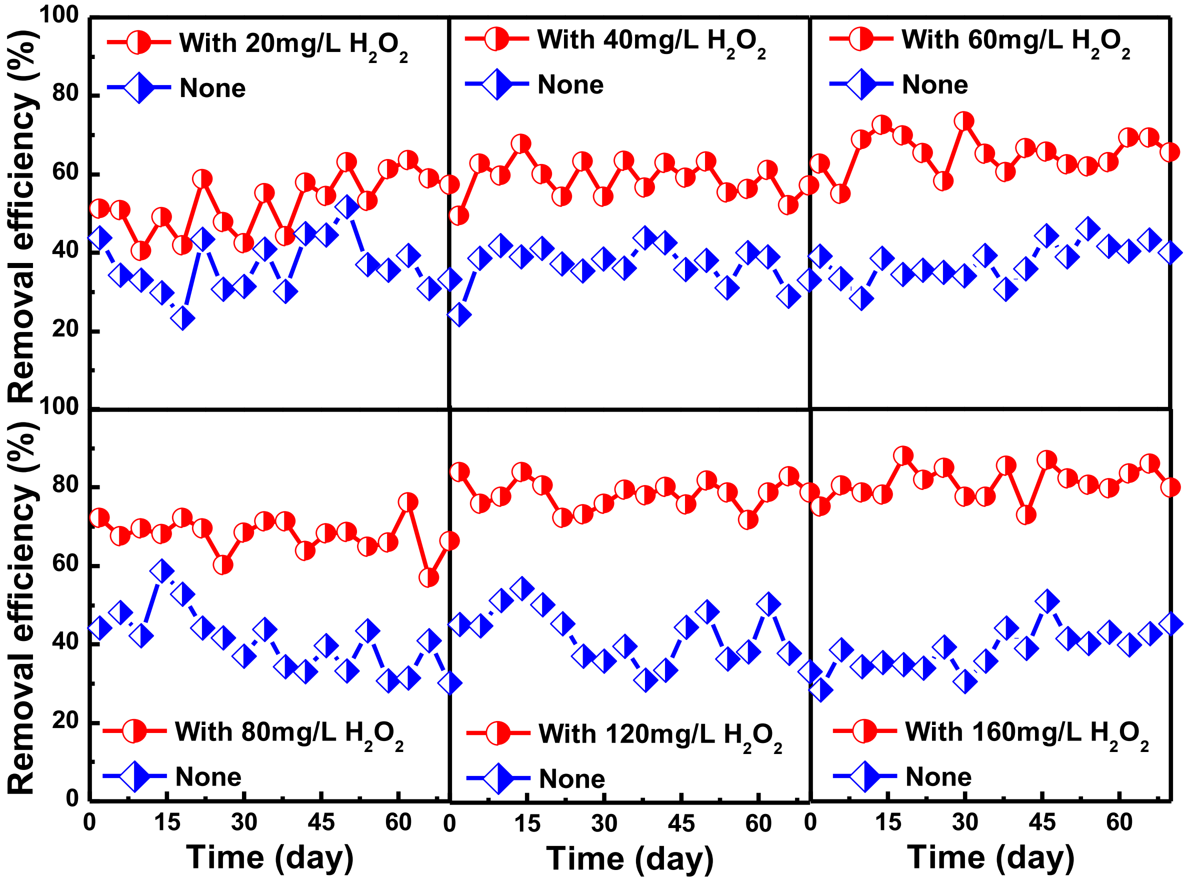
With 20mg/L H_2O_2
None
With 40mg/L H_2O_2
None
With 60mg/L H_2O_2
None
With 80mg/L H_2O_2
None
With 120mg/L H_2O_2
None
With 160mg/L H_2O_2
None
Removal efficiency (%)
Removal efficiency (%)
Time (day)
Time (day)
Time (day)
0
20
40
60
80
100
0
15
30
45
60

Fig.5

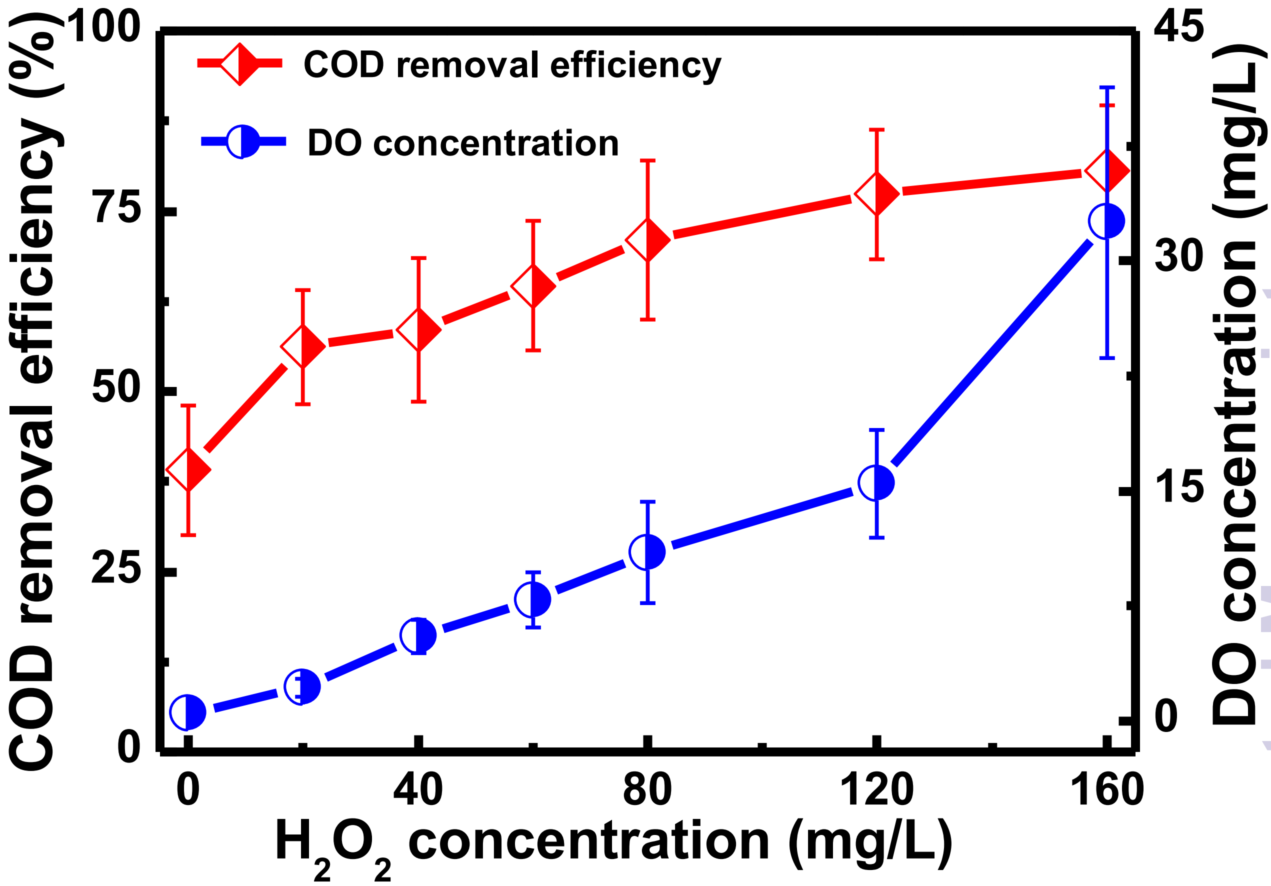
COD removal efficiency
DO concentration
COD removal efficiency (%)
DO concentration (mg/L)
H2O2 concentration (mg/L)
0
25
50
75
100
15
30
45
40
80
120
160

Fig.6

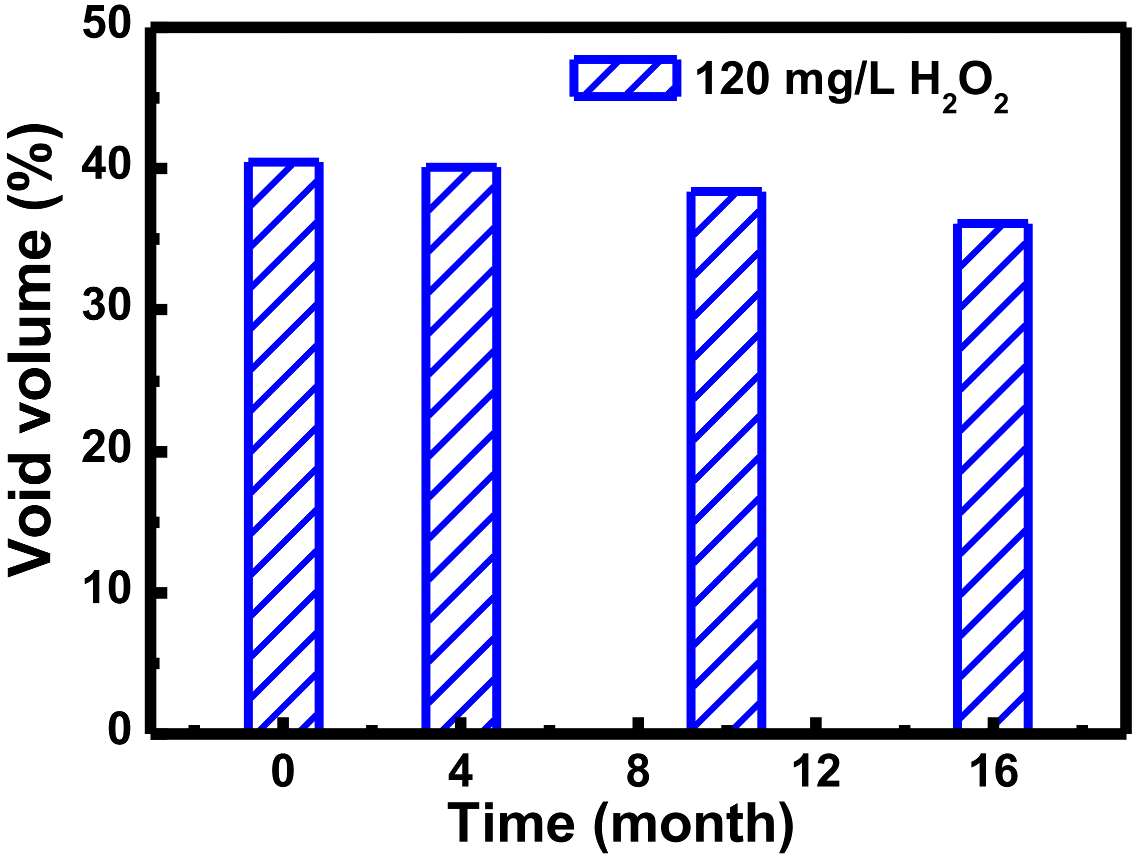

Fig.7